Research Article | Vol. 26, No. 13 | 25 Jun 2018 | OPTICS EXPRESS 16572
Optics EXPRESS

High dynamic range liquid crystal displays with a mini-LED backlight

GUANJUN TAN,[1,3] YUGE HUANG,[1,3] MING-CHUN LI,[2] SEOK-LYUL LEE,[2] AND SHIN-TSON WU[1,*]

[1]College of Optics and Photonics, University of Central Florida, Orlando, Florida 32816, USA
[2]AU Optronics Corp., Hsinchu Science Park, Hsinchu 300, Taiwan
[3]These authors contributed equally to this work
*swu@creol.ucf.edu

Abstract: We analyze the performance of high dynamic range liquid crystal displays (LCDs) using a two-dimensional local dimming mini-LED backlight. The halo effect of such a HDR display system is investigated by both numerical simulation and human visual perception experiment. The halo effect is mainly governed by two factors: intrinsic LCD contrast ratio (CR) and dimming zone number. Based on our results, to suppress the halo effect to indistinguishable level, a LCD with CR≈5000:1 requires about 200 local dimming zones, while for a LCD with CR≈2000:1 the required dimming zone number is over 3000. Our model provides useful guidelines to optimize the mini-LED backlit LCDs for achieving dynamic contrast ratio comparable to organic LED displays.

OCIS codes: (120.2040) Displays; (230.3720) Liquid-crystal devices; (330.0330) Vision, color, and visual optics; (230.3670) Light-emitting diodes.

References and links

1. H. Seetzen, L. A. Whitehead, and G. Ward, "A high dynamic range display using low and high resolution modulators," SID Symp. Dig. Tech. Papers **34**(1), 1450–1453 (2003).
2. H. Seetzen, W. Heidrich, W. Stuerzlinger, G. Ward, L. Whitehead, M. Trentacoste, A. Ghosh, and A. Vorozcovs, "High dynamic range display systems," ACM Trans. Graph. **23**(3), 760–768 (2004).
3. S. Daly, T. Kunkel, X. Sun, S. Farrell, and P. Crum, "Viewer preferences for shadow, diffuse, specular, and emissive luminance limits of high dynamic range displays," SID Symp. Dig. Tech. Papers **44**(1), 563–566 (2013).
4. R. Zhu, A. Sarkar, N. Emerton, and T. Large, "Reproducing high dynamic range contents adaptively based on display specifications," SID Symp. Dig. Tech. Papers **48**(1), 1188–1191 (2017).
5. H. Chen, R. Zhu, M. C. Li, S. L. Lee, and S. T. Wu, "Pixel-by-pixel local dimming for high-dynamic-range liquid crystal displays," Opt. Express **25**(3), 1973–1984 (2017).
6. M. Schadt, "Milestone in the history of field-effect liquid crystal displays and materials," Jpn. J. Appl. Phys. **28**(3), 03B001 (2009).
7. C. W. Tang and S. A. VanSlyke, "Organic electroluminescent diodes," Appl. Phys. Lett. **51**(12), 913–915 (1987).
8. H. Chen, J. H. Lee, B. Y. Lin, S. Chen, and S. T. Wu, "Liquid crystal display and organic light-emitting diode display: present status and future perspectives," Light Sci. Appl. **7**(3), 17168 (2018).
9. G. Tan, R. Zhu, Y. S. Tsai, K. C. Lee, Z. Luo, Y. Z. Lee, and S. T. Wu, "High ambient contrast ratio OLED and QLED without a circular polarizer," J. Phys. D Appl. Phys. **49**(31), 315101 (2016).
10. H. Chen, G. Tan, and S. T. Wu, "Ambient contrast ratio of LCDs and OLED displays," Opt. Express **25**(26), 33643–33656 (2017).
11. C. H. Oh, H. J. Shin, W. J. Nam, B. C. Ahn, S. Y. Cha, and S. D. Yeo, "Technological progress and commercialization of OLED TV," SID Symp. Dig. Tech. Papers **44**(1), 239–242 (2013).
12. S. Kobayashi, S. Mikoshiba, and S. Lim, *LCD Backlights* (John Wiley & Sons, 2009).
13. Z. Luo, Y. Chen, and S. T. Wu, "Wide color gamut LCD with a quantum dot backlight," Opt. Express **21**(22), 26269–26284 (2013).
14. P. de Greef and H. G. Hulze, "Adaptive dimming and boosting backlight for LCD-TV Systems," SID Symp. Dig. Tech. Papers **38**(1), 1332–1335 (2007).
15. H. Chen, J. Sung, T. Ha, and Y. Park, "Locally pixel-compensated backlight dimming for improving static contrast on LED backlit LCDs," SID Symp. Dig. Tech. Papers **38**(1), 1339–1342 (2007).
16. C. C. Lai and C. C. Tsai, "Backlight power reduction and image contrast enhancement using adaptive dimming for global backlight applications," IEEE Trans. Consum. Electron. **54**(2), 669–674 (2008).

#331881 https://doi.org/10.1364/OE.26.016572
Journal © 2018 Received 16 May 2018; revised 6 Jun 2018; accepted 7 Jun 2018; published 13 Jun 2018

Optics EXPRESS

17. H. Chen, T. H. Ha, J. H. Sung, H. R. Kim, and B. H. Han, "Evaluation of LCD local-dimming-backlight system," J. Soc. Inf. Disp. **18**(1), 57–65 (2010).
18. T. Shirai, S. Shimizukawa, T. Shiga, S. Mikoshiba, and K. Käläntär, "RGB-LED backlights for LCD-TVs with 0D, 1D, and 2D adaptive dimming," SID Symp. Dig. Tech. Papers **37**(1), 1520–1523 (2006).
19. H. G. Hulze and P. de Greef, "Power savings by local dimming on a LCD panel with side lit backlight," SID Symp. Dig. Tech. Papers **40**(1), 749–752 (2009).
20. S. Cha, T. Choi, H. Lee, and S. Sull, "An optimized backlight local dimming algorithm for edge-lit LED backlight LCDs," J. Disp. Technol. **11**(4), 378–385 (2015).
21. F. C. Lin, Y. P. Huang, L. Y. Liao, C. Y. Liao, H. P. D. Shieh, T. M. Wang, and S. C. Yeh, "Dynamic backlight gamma on high dynamic range LCD TVs," J. Disp. Technol. **4**(2), 139–146 (2008).
22. S. E. Kim, J. Y. An, J. J. Hong, T. W. Lee, C. G. Kim, and W. J. Song, "How to reduce light leakage and clipping in local-dimming liquid crystal displays," J. Soc. Inf. Disp. **17**(12), 1051–1057 (2009).
23. X. B. Zhang, R. Wang, D. Dong, J. H. Han, and H. X. Wu, "Dynamic backlight adaptation based on the details of image for liquid crystal displays," J. Disp. Technol. **8**(2), 108–111 (2012).
24. N. Burini, E. Nadernejad, J. Korhonen, S. Forchhammer, and X. Wu, "Modeling power-constrained optimal backlight dimming for color displays," J. Disp. Technol. **9**(8), 656–665 (2013).
25. S. X. Jin, J. Li, J. Y. Lin, and H. X. Jiang, "InGaN/GaN quantum well interconnected microdisk light emitting diodes," Appl. Phys. Lett. **77**(20), 3236–3238 (2000).
26. H. X. Jiang and J. Y. Lin, "Nitride micro-LEDs and beyond-a decade progress review," Opt. Express **21**(S3 Suppl 3), A475–A484 (2013).
27. Z. Liu, W. C. Chong, K. M. Wong, and K. M. Lau, "GaN-based LED micro-displays for wearable applications," Microelectron. Eng. **148**, 98–103 (2015).
28. H. V. Han, H. Y. Lin, C. C. Lin, W. C. Chong, J. R. Li, K. J. Chen, P. Yu, T. M. Chen, H. M. Chen, K. M. Lau, and H. C. Kuo, "Resonant-enhanced full-color emission of quantum-dot-based micro LED display technology," Opt. Express **23**(25), 32504–32515 (2015).
29. J. Korhonen, N. Burini, S. Forchhammer, and J. M. Pedersen, "Modeling LCD displays with local backlight dimming for image quality assessment," Proc. SPIE **7866**, 843607 (2011).
30. Z. Deng, B. Zheng, J. Zheng, L. Wu, W. Yang, Z. Lin, P. Shen, and J. Li, "High dynamic range incell LCD with excellent performance," SID Symp. Dig. Tech. Papers **49**(1), 996–998 (2018).
31. R. Hunt and M. R. Pointer, *Measuring Colour*, 4th ed. (Wiley, 2011).
32. M. D. Fairchild, *Color Appearance Models*, 3rd ed. (Wiley, 2013).
33. D. Zwillinger and S. Kokoska, *CRC Standard Probability and Statistics Tables and Formulae* (Chapman & Hall/CRC, 2000).
34. D. M. Hoffman, N. N. Stepien, and W. Xiong, "The importance of native panel contrast and local dimming density on perceived image quality of high dynamic range displays," J. Soc. Inf. Disp. **24**(4), 216–228 (2016).

1. Introduction

High dynamic range (HDR) is an important feature for next generation displays [1,2]. A HDR display must exhibit a high contrast ratio (CR>10^5:1) in order to reveal the detailed images in both high and low brightness regions simultaneously. To achieve HDR, high peak brightness and excellent dark state of the display system are required [3, 4]. For instance, the luminance of the bright state should exceed 1000 nits, while the dark state should be below 0.01 nits [5]. Nowadays, liquid crystal display (LCD) [6] and organic light-emitting diode (OLED) [7] are two leading display technologies [8]. However, both OLEDs and LCDs need substantial improvements to realize the HDR features. First of all, OLED is an emissive display, as a result, it is relatively easy to display true black state [9, 10]. However, to achieve a brightness over 1000 nits would require a relatively high current, which would compromise the lifetime [8, 11]. On the other hand, LCD is a non-emissive display and requires a backlight unit, such as white light emitting diode (LED) [12] or blue LED pumped quantum dots [13]. A major advantage of LCD is that it can achieve high brightness (>1000 nits) by cranking up the LED luminance. However, a pitfall is its limited contrast ratio (CR), which depends on the liquid crystal alignment. For example, a commercial multi-domain vertical alignment (MVA) LCD, mainly used in TVs, can provide CR≈5000:1, which is still 20 × lower than the HDR requirement. Therefore, how to achieve HDR is becoming a significant and urgent task for LCD. To overcome this challenge, segmented LEDs are adopted in the LCD backlight unit, where the local zones can be independently dimmed to match the displayed image contents [14–20]. This so-called *local dimming* technique can effectively suppress the dark state light leakage and greatly enhance the contrast ratio. Both direct-lit type [5, 14–17] and edge-lit type [18–20] local dimming backlight systems have been developed. Direct-lit type local

Optics EXPRESS

dimming exhibits better HDR performance, while edge-lit type backlight offers a thinner profile [19, 20]. A common issue of local dimming, no matter direct-lit or edge-lit, is the *halo effect*. The halo artifact usually appears around a bright object on dark background due to light leakage of the LCD panel. Extensive efforts on how to improve the image quality by backlight dimming algorithms have been conducted [2, 21–24]. From the device viewpoint, higher intrinsic LCD contrast ratio and appropriate local dimming zones are two promising approaches.

Recently, micro-LED and mini-LED have attracted much attentions. Micro-LED with a chip size less than 100 μm is considered as a revolutionary technology for future displays [25–28]. However, the manufacturing yield of micro-LED mass transfer remains a big challenge. On the other hand, mini-LED has a larger chip size (100~500 μm) than micro-LED and its fabrication is also much easier. Thus, mini-LED is an ideal backlight candidate to enable local dimming for LCDs. In addition to high brightness (>1000 nits), mini-LED backlight can provide more than 10,000 local dimming zones to achieve excellent HDR performance. What is more, due to the small dimension of mini-LED, it can offer freeform outline and narrow bezel, which is highly desirable for smartphone applications. Until now, there is no detailed discussion on system modeling and performance evaluation of LCDs with mini-LED backlight.

In this paper, we develop a numerical model to analyze and optimize the HDR LCD system with a mini-LED backlight. The proposed model is capable of analyzing the whole display system from mini-LED backlight, diffuser to LC panel, and finally producing full-color images displayed by the system. Peak Signal to Noise Ratio (PSNR) in the CIE 1976 *L*a*b** color space is selected as the metric to evaluate HDR performance, mainly the halo effect. Based on this model, the impacts of local dimming zone number and intrinsic LCD CR are investigated respectively. Then, subjective perception experiments are designed and carried out to determine the human visual perception limit for HDR contents. Our results indicate that a LCD with CR≈5000:1 (MVA TV) would require >200 dimming zones to achieve unnoticeable halo effect. While for a LCD with CR≈2000:1, the required dimming zones is over 3000.

2. Device modelling

2.1 Simulation model and verification

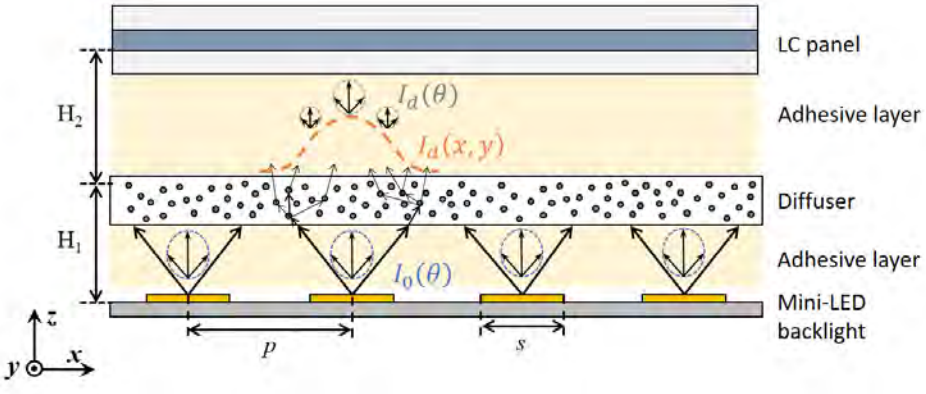

Fig. 1. Schematic diagram of the LCD display with a mini-LED backlight.

Figure 1 depicts the device structure of the LCD system with a direct-lit mini-LED backlight, which is not drawn to scale. The backlight unit consists of square-shaped mini-LED array with chip size *s* and pitch length *p*. For simplicity, we assume that all the mini-LEDs having the same angular emission pattern $I_0(\theta)$. Of course, different emission patterns can be applied

for different application needs. Without losing generality, *Lambertian* emission is adopted in our simulation. Then a diffuser plate is applied to spread the light to obtain good spatial uniformity. In our simulation, we used the point spread function (PSF) theory [24, 29] to model the light propagation from mini-LED backlight to LCD panel. The diffuser plate is utilized to widen both spatial and angular distributions. The bidirectional scattering distribution function (BSDF) can be used as an accurate description of the diffuser plate. Here we can make a reasonable simplification. The angular distribution of the light travelling through the diffuser is described as $I_d(\theta)$. Also, we assume that $I_d(\theta)$ follows *Lambertian* distribution, i.e. $I_d(\theta) \propto \cos(\theta)$, for a strong diffuser. Moreover, this assumption also applies to color conversion film, for instance phosphor or quantum-dot layer. The widened spatial distribution follows 2-D Gaussian function as:

$$I_d(x, y) = \exp\left[-\frac{(x-x_0)^2 + (y-y_0)^2}{2\rho^2}\right], \quad (1)$$

where (x_0, y_0) is the location of incident source point and ρ is the standard deviation of the spatial distribution. The standard deviation ρ can be tuned to achieve good spatial uniformity.

In our simulations, the system settings are based on the device configuration reported in [30]. The dimensions of mini-LED array are p = 1 mm and s = 0.5 mm. The effective light diffusion distances, by considering substrates and adhesive layers between backlight, diffuser plate and LCD panel are set as H_1 = 0.4 mm and H_2 = 0.5 mm in order to obtain good spatial uniformity. Then we simulate a 6.4-inch 2880 × 1440 LCD system with mini-LED backlight. The diffusion standard deviation ρ in Eq. (1) is adjusted to be ρ = 0.4 mm in order to generate uniform luminance over the whole display panel. Typically, the edge of the backlight would be dimmer than the central region. Thus, we also set the backlight area (146 mm × 74 mm) slightly larger than the LCD panel (144 mm × 72 mm) to assure an excellent uniformity.

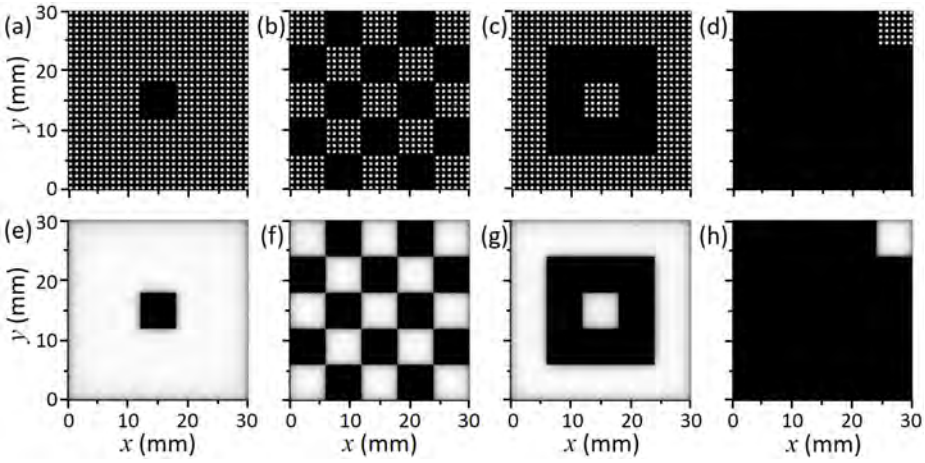

Fig. 2. Mini-LED backlight local dimming modulation with (a) pattern I, (b) pattern II, (c) pattern III, and (d) pattern IV. Simulated displayed images: (e) pattern I, (f) pattern II, (g) pattern III, and (h) pattern IV.

To validate our model, we simulated the abovementioned display system with local dimming effect, and then compared our results with the experimental data reported in [30]. According to [30], the backlight consists of 24 × 12 local dimming zones and each zone has 6 × 6 mini-LEDs, which can be modulated independently. The employed in-plane switching (IPS) LCD panel has a CR≈1500:1. We investigated four test patterns, as Figs. 2(a)-2(d) show, and calculated the corresponding dynamic contrast ratios. Figures 2(e)-2(h) show their corresponding displayed patterns. Table 1 compares the calculated dynamic CRs.

Optics EXPRESS

From Table 1, our simulated results agree with the measured data from [30] reasonably well. It should be mentioned that for such a high CR measurement, the black state is approaching the noise level of the employed photodiode detector. Thus, some variation in the measured CR is expected.

Table 1. Simulated and measured [30] dynamic contrast ratios of four test patterns.

Pattern	I	II	III	IV
Simulated CR	15,094	46,547	32,245	31,590,212
Measured CR	~20,000	25,000~40,000	25,000~40,000	>3,000,000

2.2 Displayed image simulation and evaluation metric

As described above, our simulation model can predict the dynamic contrast ratio of a display system. While a complete simulation model should be able to simulate the displayed images and then to evaluate the HDR performance. Thus, our following work is to further develop the model to simulate the final displayed images. The target is to make our model capable of relating the device structure to the final HDR display performance, especially the halo effect.

As to the displayed image simulation, first we need to determine how to modulate the mini-LED backlight and LCD panel, respectively. Since our main focus here is on the halo effect, we use the Max-algorithm [2] and LC pixel compensation [29] to minimize the clipping effect. As for a target image to be displayed using our system, we first divide the image into several zones according to the backlight local dimming zones. Within each zone, the maximum luminance of the target image is used to determine the luminance of the corresponding mini-LED backlight zone. With the proposed simulation model, the luminance distribution of the light incident on the LC layer can be calculated. Then we can determine the LC panel's transmittance by the ratio between the luminance on the LC layer and that of the target image. The LED backlight modulation depth is reasonably set to be 10 bits while the LC panel transmittance modulation is 8 bits. Here we give an example of 'Candle' image in the dark background, as illustrated in Fig. 3. The mini-LED backlight modulation is depicted in Fig. 3(a), and the simulated luminance distribution incident on the LC layer is presented in Fig. 3(b). By considering the LC panel modulations through R/G/B channels respectively, we can obtain the final displayed full-color image, as Fig. 3(c) shows.

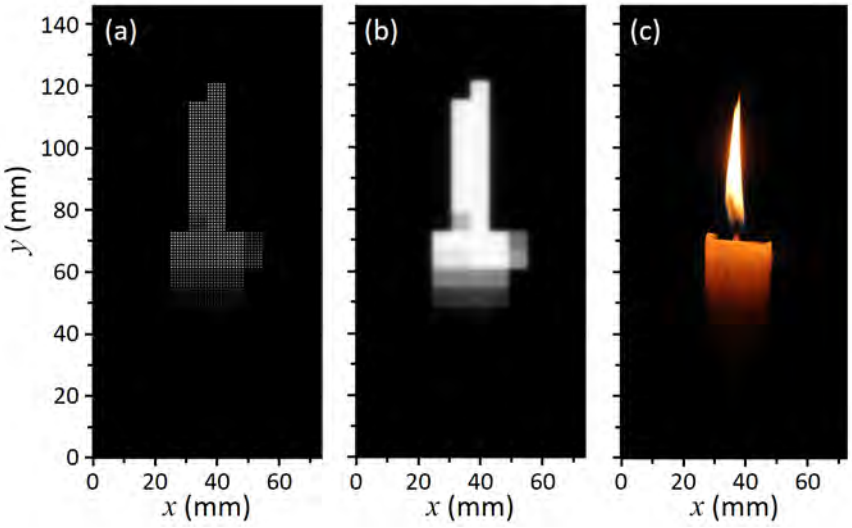

Fig. 3. Displayed image simulation: (a) Mini-LED backlight modulation; (b) luminance distribution of the light incident on LC layer, and (c) displayed image after LCD modulation.

Optics EXPRESS

Although it is not easy to observe, the halo around the bright candle area still exists in Fig. 3(c), due to the light leakage of LC panel (CR~1500:1). An evaluation metric is needed to evaluate the halo effect quantitatively. In our analysis, both brightness and color need to be taken into consideration. Therefore, Peak Signal-to-Noise Ratio (PSNR) in the CIE 1976 *L*a*b** color space can be used in our evaluations. The conventional CIE 1931 XYZ coordinates can be easily converted to *L*a*b** color space by [31, 32]:

$$\begin{aligned} L^* &= 116 f\left(Y/Y_n\right) - 16 \\ a^* &= 500\left[f\left(X/X_n\right) - f\left(Y/Y_n\right)\right], \\ b^* &= 200\left[f\left(Y/Y_n\right) - f\left(Z/Z_n\right)\right] \end{aligned} \tag{2}$$

where

$$f(t) = \begin{cases} \sqrt[3]{t}, & \text{if } t > \left(6/29\right)^3 \\ \dfrac{t}{3\times\left(6/29\right)^2} + \dfrac{4}{29}, & \text{otherwise} \end{cases}. \tag{3}$$

In the LAB color space, L^* represents the lightness value, a^* represents the green-red component, and b^* represents the blue-yellow component. And the X_n, Y_n and Z_n in Eq. (2) are the XYZ values of the reference white, respectively. Based on Eq. (2), we can define the color difference in *L*a*b** color space, which is the perceived difference between two colors, considering both luminance and chrominance differences [31,32]:

$$\Delta E = \sqrt{\Delta L^{*2} + \Delta a^{*2} + \Delta b^{*2}}, \tag{4}$$

where ΔL^*, Δa^*, and Δb^* are the differences between the displayed image and target image. With that, we can define *LabPSNR* by following equation [24]:

$$LabPSNR = 10\times\log_{10}\left[\frac{\left(\Delta E_{\max}\right)^2}{\dfrac{1}{mn}\sum_{i=1}^{n}\sum_{j=1}^{m}\Delta E\left(i,j\right)^2}\right], \tag{5}$$

where m and n are the image resolution (2880 × 1440 in our example) and $\Delta E_{\max}$ is the difference between black and white. In our simulations, the normalized $\Delta E_{\max}$ is set to be 100. Then with *LabPSNR* as the evaluation metric, we are able to quantify the difference between displayed image and target image.

In Fig. 3, the backlight has only 288 local dimming zones and the LCD contrast ratio is 1500:1. In the following simulations, we will discuss how the local dimming zone number and LCD contrast ratio influence the final display performance. The Candle image is used again as an example. The *L*a*b** color difference ΔE of the displayed images with different local dimming zones are presented in Fig. 4. The contrast ratios in Fig. 4 are all kept at 1500:1. From Figs. 4(a) to 4(d), the number of local dimming zones is 18, 288, 1152 and 10368, respectively. The corresponding mini-LED number in each zone is 24 × 24, 6 × 6, 3 × 3 and 1 × 1. From Figs. 4(a)-4(d), we can find a clear trend: the displayed image distortion decreases as the local dimming zone number increases. Especially, the halo area around the bright candle dramatically decreases. The calculated *LabPSNR* is improved from 39.9 dB to 48.8 dB as well.

Optics EXPRESS

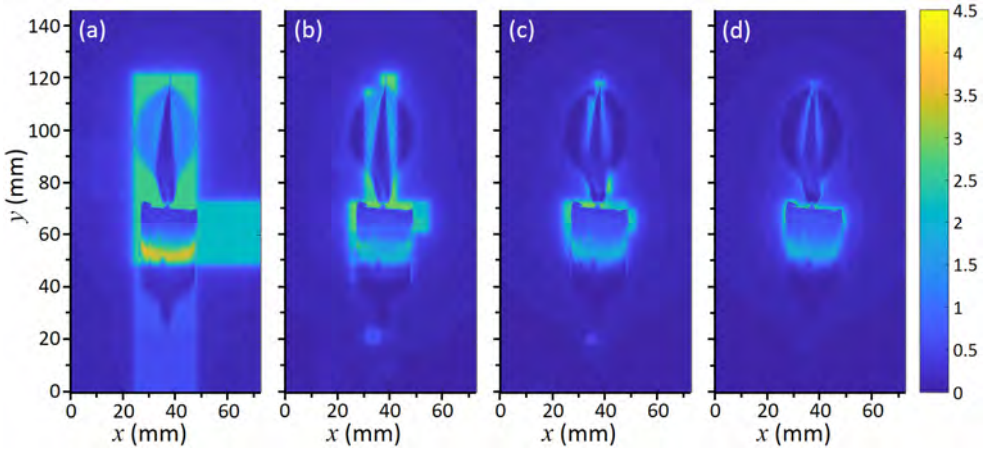

Fig. 4. The $L^*a^*b^*$ color difference ΔE between target and displayed images with different local dimming zone numbers: a) 18; b) 288; c) 1152 and d) 10368.

Besides the local dimming zone number, LCD contrast ratio is another important factor affecting the final HDR performance. Therefore, we also analyze the influence of intrinsic LCD contrast ratio. Figure 5 shows the simulated ΔE of the displayed images with CR increasing from 1500:1 to 4500:1. The local dimming zone number is set to be 1152 in the simulations illustrated in Fig. 5. As depicted in Figs. 5(a)-5(d), the halo area does not change while the color distortion ΔE value decreases as the LC contrast ratio increases. In addition, *LabPSNR* increases from 46.9 dB [Fig. 5(a)] to 51.6 dB [Fig. 5(d)]. From Fig. 4 and Fig. 5, the impacts of local dimming zone number and LCD contrast ratio can be distinguished. The dimming zone number mainly affects the halo area, while LCD contrast ratio influences the local image distortion.

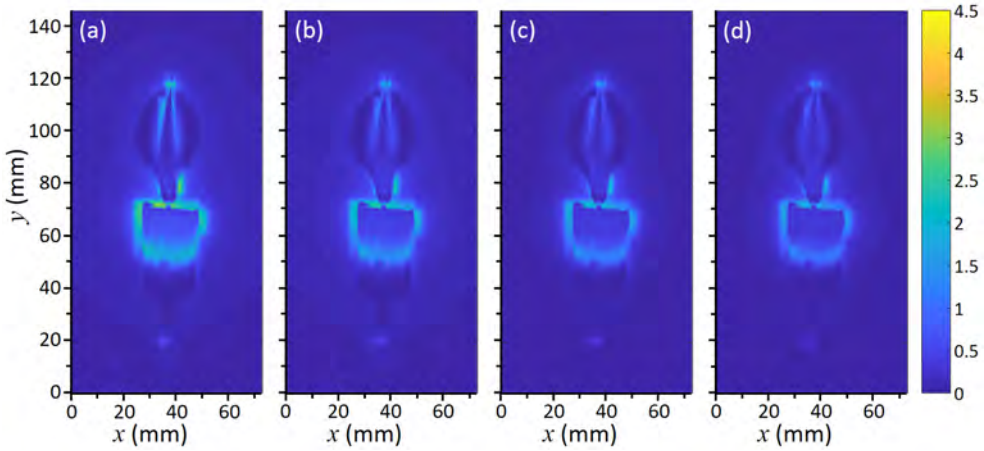

Fig. 5. The $L^*a^*b^*$ color difference ΔE between target and displayed images with LCD contrast ratios: a) 1500:1; b) 2500:1; c) 3500:1 and d) 4500:1.

3. Subjective experiment

As discussed above, more local dimming zones and higher LC contrast ratio can reduce the halo effect and improve the display performance. However, the minimum number for dimming zones and LC contrast ratio have not been clearly quantified. In this section, a subjective experiment is designed and carried out to measure human visual perception limit of

Optics EXPRESS

halo effect. With visual perception limit obtained, the required local dimming zone number for an ideal HDR display with indistinguishable halo effect could be estimated.

Ten images were employed in our experiment. As shown in Fig. 6, all of the pictures have highlight spots and dark areas qualifying the HDR content requirement. In the meantime, the diversity of the image content was also considered. Some pictures are generally bright [Figs. 6(a), 6(c), and 6(g)], while some have a large portion of dark areas [Figs. 6(d), 6(f) and 6(j)]. Moreover, in Figs. 6(b), 6(d) and 6(f), the high-luminance pixels are finely disseminated in the dark background. While in Figs. 6(c) and 6(h)-6(j), there are relatively concentrated bright and dark blocks.

Fig. 6. HDR target pictures used in the subjective experiment: a) Beach, b) City light, c) Christmas, d) Firework, e) Tower, f) Stars, g) Sunset, h) Waffle house, i) Lamp, and j) Candle.

3.1 Image rendering

Based on the model described in previous section, we simulated the displayed images by LCD systems with mini-LED backlight. Ten different local dimming zone numbers (1, 2, 8, 18, 72, 288, 648, 1152, 2592 and 10368) and seven LC contrast ratios (1000:1, 1500:1, 2000:1, 3000:1, 4000:1, 4500:1 and 5000:1) were applied to each picture, generating seventy different rendering conditions in total. In the following experiment, 70 simulated images were selected covering all the rendering conditions. Diverse image contents were evenly distributed in different number of local dimming zones and different LC contrast ratios.

Optics EXPRESS

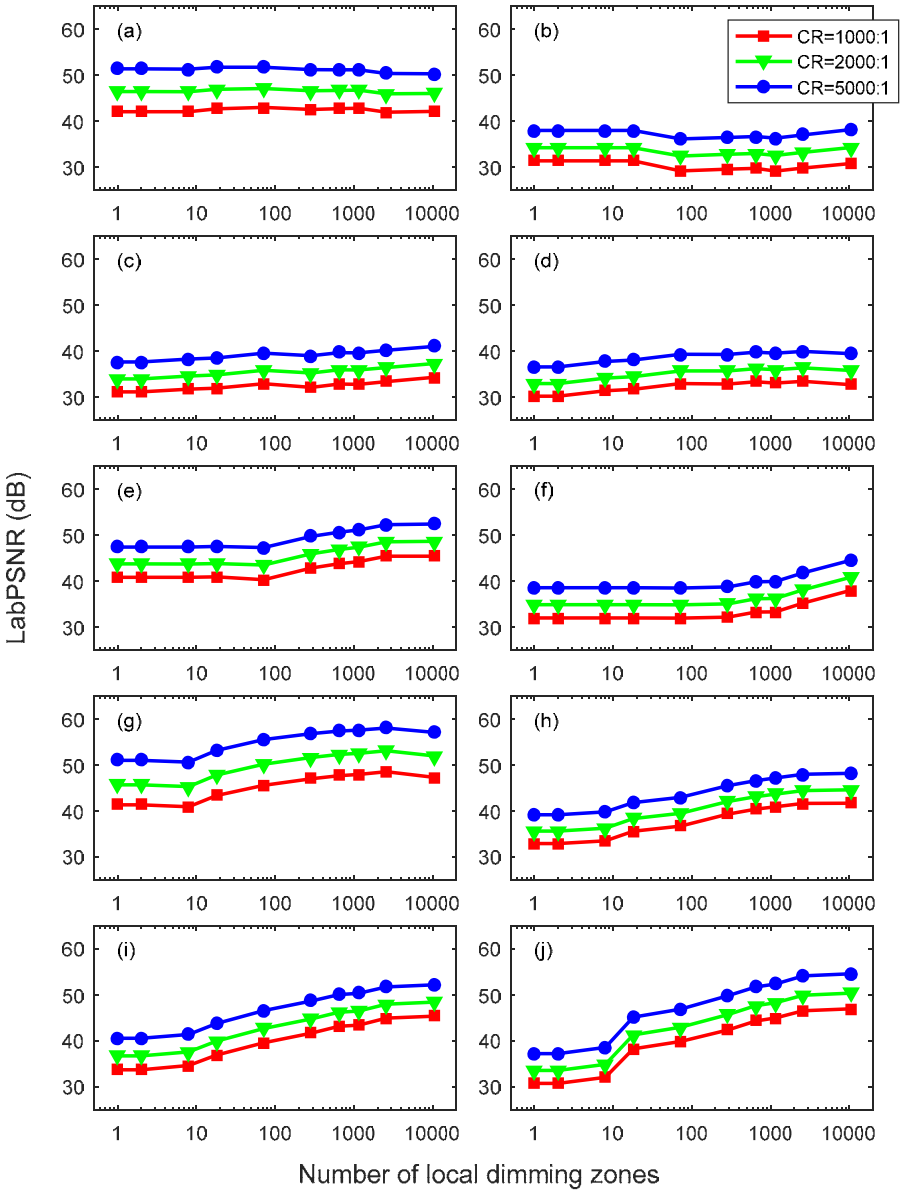

Fig. 7. Simulated *LabPSNR* with various local dimming zone numbers and LC contrast ratios for 10 images: a) Beach, b) City light, c) Christmas, d) Firework, e) Tower, f) Stars, g) Sunset, h) Waffle house, i) Lamp, and j) Candle.

The *LabPSNR* of each simulated image displayed by various local dimming zones and LC contrast ratios was calculated and presented in Fig. 7. We can see, even under the same rendering condition, the *LabPSNR* of simulated images are actually different for various image contents. For all of the ten pictures, *LabPSNR* increases as the LC contrast ratio increases. About 7.2 dB increase can be obtained from the contrast ratio change from 1000:1 to 5000:1. With local dimming zone increases, the image quality degradation of the displayed image is expected to decrease, namely a larger *LabPSNR* value. From Fig. 7, we notice that for certain pictures, *LabPSNR* value increases dramatically [Figs. 7(h)-7(j)]. While, for other images [Figs. 7(a)-7(d)], the increasing trend is not so obvious. The *LabPSNR* improvement

depends on the image contents. This is actually related to the mixability of the bright and dark pixels in the images. For the pictures with well-mixed bright and dark pixels [Fig. 6(a), 6(b) and 6(d)], when the size of local dimming zone is much larger than the uniform-luminance block size, the help of increased local dimming zone number would be limited.

3.2 Experimental setup

Eleven people with normal or corrected normal vision participated in this experiment. Their ages range from 22 to 28 years old with an average value of 25.5. The experiment was carried out on each observer independently. In a dark room, two OLED panels (Samsung Galaxy S8, panel size 5.8", resolution 2960x1440) were placed at 25 cm (least distance of distinct vision) away from the observer's eyes. One of the OLED panels displays a simulated displayed image by a mini-LED-backlit LCD system while the other displays the original target image. The observers were asked to select the image they preferred between the two displayed images. In total, seventy sets of image pairs were displayed to each observer. To avoid the influence of prejudgment and viewing angle, the target images were randomly displayed on one of the smartphones between different sets of image pairs, and the location of two smartphones was exchanged for different observers.

3.3 Results

Figure 8 shows the experimental results. The perceived difference stands for the ratio of observers who are able to distinguish the target images from the simulated displayed images by the mini-LED-backlit LCD system. The *LabPSNR* values of the 70 rendered images scatter over a wide range. In Fig. 8, the yellow bars denote the averaged perceived difference ratio in each *LabPSNR* range and the black error bars mark the standard deviation of the experimental data.

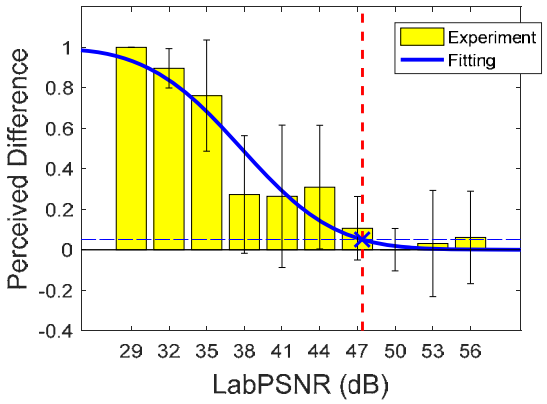

Fig. 8. Subjective experiment results of perceived image difference versus *LabPSNR* of the images.

In our fitting, we assume the observers can only perceive the difference between two images whose *LabPSNR* is lower than a critical value, noted as $LabPSNR_{cri}$. Here, $LabPSNR_{cri}$ could vary depending on different viewers, and its probability density (f) follows normal distribution:

$$f\left(LabPSNR_{cri}\right)=\frac{1}{\sigma\sqrt{2\pi}}e^{-\frac{\left(LabPSNR_{cri}-\mu\right)^2}{2\sigma^2}}, \tag{6}$$

where μ is the expectation of $LabPSNR_{cri}$ and σ is the standard deviation. For a given image pair with different *LabPSNR*, the probability that observers cannot perceive the difference follows cumulative distribution function [33]:

$$F\left(LabPSNR\right) = \text{Prob}\left[LabPSNR_{cri} \le LabPSNR\right] = \int_{-\infty}^{LabPSNR} f\left(LabPSNR_{cri}\right) d\,LabPSNR_{cri}. \quad (7)$$

Therefore, the perceived difference should follow 1–*F*(*LabPSNR*), which was used to fit the experimental data. The fitting curve is plotted as the blue solid line in Fig. 8. From the fitting result, for a displayed image with *LabPSNR* > 47.4 dB, only less than 5% of the observers could perceive the difference between the displayed and target images. The good match between fitting curve and experimental data implies that *LabPSNR* could be used to predict the human perceptibility of the displayed images.

Having obtained the required *LabPSNR* value, our next step is to evaluate the requirements of the display system. From Fig. 7, it is denoted that the improvement by local dimming technology is dependent on the image content. It is undeniable that as for certain images with a large portion of high spatial frequency component, pixel-level local dimming is necessary for faithful reproduction. However, for most HDR contents, local dimming technology helps greatly. Therefore, in our discussion, we mainly focus on the cases in which local dimming works effectively. Figure 9 plots the average *LabPSNR* values of the pictures with obvious display quality improvement. As expected, *LabPSNR* can be improved by increasing dimming zone number and LCD's contrast ratio. Let's use 47.4 dB as the criterion to estimate the required dimming zone number. If a LCD with CR≈1000:1, then even 10,000 local dimming zones is still inadequate. For a LCD with CR≈2000:1, (e.g., fringing-field switching (FFS) LCD), the required local dimming zones is reduced to 3000. If a LCD with CR = 5000 (e.g. MVA), then an unnoticeable halo effect can be achieved at ~200 local dimming zones. Our obtained results are consistent with the experimental data reported [34]. Our work sheds new light for optimizing the HDR displays with mini-LED backlit LCDs.

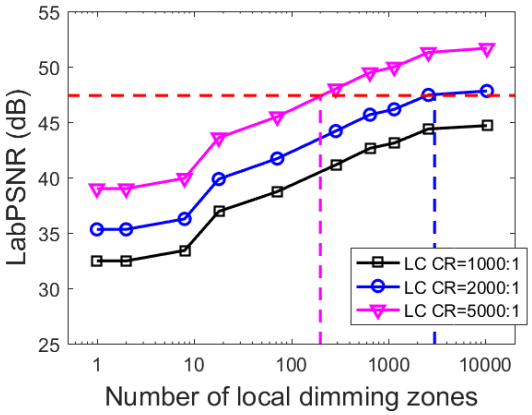

Fig. 9. Simulated *LabPSNR* for different HDR display systems with various local dimming zone numbers and LC contrast ratios.

4. Discussion

In above sections, our simulations and experiments are all based on the small-size smartphone displays with viewing distance at 25 cm. Actually our analysis and conclusion can also be applied to display devices with different sizes and resolutions. The basic concept is to convert our results from spatial domain to angular domain. For example, based on our settings of a

6.4 inch mobile display at 25-cm viewing distance, ~200 local dimming zones is needed for an LCD with CR = 5000:1. Under such a condition, the angular distance of two adjacent local dimming zones is calculated to be θ_z = 1.65°. That is to say, for human eyes, the required angular density of local dimming zones should be over 0.606 zones per degree (ZPD). Based on this information, we are able to scale up the display size and resolution, as shown in Fig. 10.

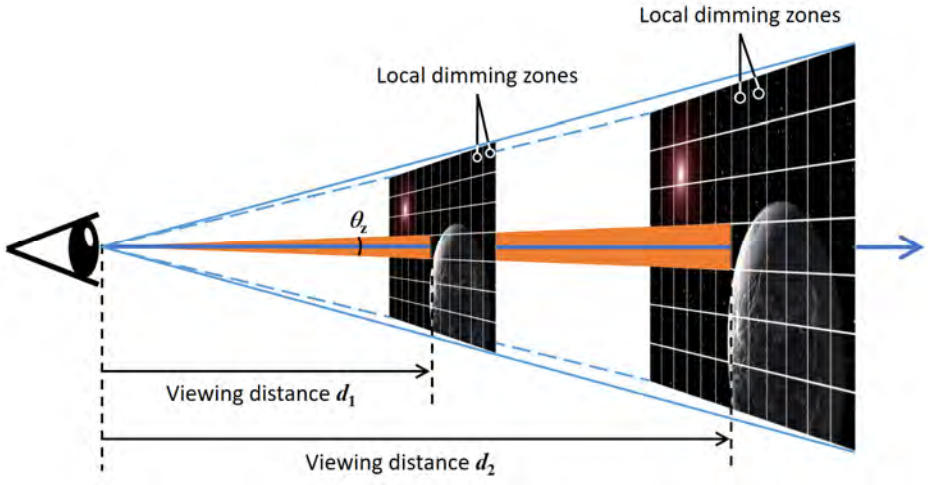

Fig. 10. Conceptual diagram of scaling up display size based on same angular size.

Here we give two examples of large size MVA panels with CR = 5000:1: 1) 65-inch TV with 4K (3840 × 2160) resolution and 2) 85-inch TV with 8K (7680 × 4320) resolution. Because the human-perceived display performance depends on the viewing distance from the panel to the observer, here, we consider two scenarios. The first case is the *minimum viewing distance* calculated by an angular pixel density of 60 pixels per degree (PPD), which corresponds to the human visual acuity of 1 arcmin for a normal person with 20/20 vision. As shown in Table 2, the calculated minimum viewing distance is 1.29 m for the 65-inch 4K TV and 0.84 m for the 85-inch 8K TV. We find that the required dimming zone number for the 8K TV (3432 zones) is four times higher than that of the 4K TV (858 zones). The reason is that under the same angular pixel density the pixel number in one dimming zone is fixed as: (60 PPD / 0.606 ZPD)^2 = 99^2 pixels per zone. Therefore, the required zone number is proportional to the panel pixel number. The second distance considered here is the *optimum viewing distance*, at which the display occupies a 40° field of view (FOV) for the viewer. As demonstrated in Fig. 10 and Table 2, regardless of the panel size and resolution, the two panels occupying the same FOV have the same requirement on dimming zone number (364 zones). Another information extracted from Table 2 is that a shorter viewing distance usually requires more local dimming zones due to more distinguishable details.

Table 2. Required local dimming zone numbers for large size TVs.

65” 4K TV (3840 × 2160)				85” 8K TV (7680 × 4320)			
Viewing distance	FOV	PPD	Required zones	Viewing distance	FOV	PPD	Required zones
1.29 m	58.4°	60.0	~858	0.84 m	96.3°	60.0	~3432
1.98 m	40.0°	92.1	~364	2.59 m	40.0°	184.1	~364

In the previous discussion we suggested the minimum numbers of local dimming zones. However, a larger zone number is always preferred for different observers and different

viewing environment. The maximum number of local dimming zones is determined by the number of mini-LED chips. More mini-LED chips with smaller pitch length enables more dimming zones, which help reduce the halo effect. Moreover, it requires a shorter propagation distance to obtain good luminance uniformity. That means, the backlight unit is thinner. However, the associated challenges are twofold: thermal management and manufacturing difficulty. Therefore, an appropriate amount of mini-LED chips and dimming zones should be carefully selected.

5. Conclusion

In this work, we built a simplified model for LCD system with mini-LED backlight. The simulated results match well with measured data. Based on our model, we simulated the displayed image on a mini-LED backlit LCD panel, and evaluated the halo effect by the metric *LabPSNR*. By increasing the LC contrast ratio and increasing the number of local dimming zones, the halo effect can be reduced and higher image fidelity can be achieved. A subjective experiment was designed and carried out, to determine the human visual perception limit of halo effect: *LabPSNR* ~47.4 dB. Based on that limit, we can propose the requirements of local dimming zone number: over 200 local dimming zones for high CR ≈5000:1 (MVA) LCD panels, and more than 3000 dimming zones for CR ≈2000:1 (FFS) LCDs. This work paves the way to achieve excellent HDR display with mini-LED backlit LCD panels.

Funding

a.u.Vista, Inc.

Acknowledgments

The authors would like to thank Yun-Han Lee, Juan He, Jianghao Xiong, Huiyuan Liu, Tao Zhan, Kun Yin, Ziqian He, Suyuan Chen, Hao Chen and Yuanhang Zhang for participating in the subjective experiment tests, and Zhuo Deng and Dr. Yung-Hsun Wu for useful discussion. The UCF group is indebted to a.u.Vista, Inc. for financial support.